Journal of Biomechanics 148 (2023) 111472

Contents lists available at ScienceDirect

Journal of Biomechanics

journal homepage: www.elsevier.com/locate/jbiomech

Toward defining the role of the synovium in mitigating normal articular cartilage wear and tear

Matthew J. Pellicore [a], Lianna R. Gangi [a], Lance A. Murphy [a], Andy J. Lee [a], Timothy Jacobsen [a], Hagar M. Kenawy [a], Roshan P. Shah [b], Nadeen O. Chahine [a,b], Gerard A. Ateshian [b,c], Clark T. Hung [a,b,*]

[a] Department of Biomedical Engineering, Columbia University, New York, NY, USA
[b] Department of Orthopedic Surgery, Columbia University, New York, NY, USA
[c] Department of Mechanical Engineering, Columbia University, New York, NY, USA

ARTICLE INFO

Keywords:
Cartilage
Synovium
Stem cell
Mechanobiology

ABSTRACT

Cartilage repair has been studied extensively in the context of injury and disease, but the joint's management of regular sub-injurious damage to cartilage, or 'wear and tear,' which occurs due to normal activity, is poorly understood. We hypothesize that this cartilage maintenance is mediated in part by cells derived from the synovium that migrate to the worn articular surface. Here, we demonstrate *in vitro* that the early steps required for such a process can occur. First, we show that under physiologic mechanical loads, chondrocyte death occurs in the cartilage superficial zone along with changes to the cartilage surface topography. Second, we show that synoviocytes are released from the synovial lining under physiologic loads and attach to worn cartilage. Third, we show that synoviocytes parachuted onto a simulated or native cartilage surface will modify their behavior. Specifically, we show that synoviocyte interactions with chondrocytes lead to changes in synoviocyte mechanosensitivity, and we demonstrate that cartilage-attached synoviocytes can express *COL2A1*, a hallmark of the chondrogenic phenotype. Our findings suggest that synoviocyte-mediated repair of cartilage 'wear and tear' as a component of joint homeostasis is feasible and is deserving of future study.

1. Introduction

Articular cartilage is the specialized connective tissue that covers the bony ends of diarthrodial joints and serves load-bearing and lubrication functions. In most individuals, articular cartilage functions normally for many decades before beginning to break down when joint degeneration and osteoarthritis (OA) develop. In moderately active populations, activities of daily living typically involve 5000 steps of walking per day, or approximately-two hours of cyclical loading of lower extremity joints, adding up to 1.8 million cycles of loading per year and more than 108 million cycles over a 60-year lifespan. Normal 'wear and tear' of cartilage (i.e., mechanical tissue degradation without injurious loading) is anticipated (Oungoulian et al., 2015) and is accompanied by loss of chondrocytes, as reported in rabbits (Horisberger et al., 2012; Roemhildt et al., 2012). However, cartilage load-bearing is unaffected by this process, presumably due to a balance between local tissue damage and repair mechanisms which are not well understood.

Much attention is paid to dysregulation of cartilage in disease and injury rather than on mechanisms underlying its normal maintenance. As cartilage can survive for decades and perform its load-bearing and lubrication functions without issue, primary OA could then be explained by a breakdown of this homeostatic process. Recent studies have demonstrated that normal wear and tear initiates in the cartilage superficial zone (SZ) (Neu et al., 2010; Oungoulian et al., 2015). SZ chondrocytes are more vulnerable to sustained mechanical loading than other zonal chondrocytes due to the compressive (Schinagl et al., 1997) and shear (Buckley et al., 2008) properties of the SZ and heightened SZ chondrocyte susceptibility to mechanical injury (Chahine et al., 2007; Clements et al., 2001). Based on these findings, we propose that the cartilage SZ is the main target of the normal, day-to-day cartilage repair process and that this maintenance is performed by cells from the synovium (Hunziker and Rosenberg, 1996; Kurth et al., 2011; Roelofs et al., 2017). These synovial cells may bind to the slightly-degraded articular surface, differentiate into a chondrogenic lineage to replace necrotic and

* Corresponding author.
E-mail address: cth6@columbia.edu (C.T. Hung).

https://doi.org/10.1016/j.jbiomech.2023.111472
Accepted 24 January 2023
Available online 26 January 2023

apoptotic SZ chondrocytes, and repair the disrupted tissue.

The synovium is a semi-permeable, size-selective membrane that is the main barrier to the transport of molecules in synovial fluid and plasma into and out of the synovial joint. It is comprised of primarily fibroblast-like synoviocytes (FLS) within an extracellular matrix (ECM) composed of primarily hyaluronic acid (HA), collagen, and proteoglycans (Hui et al., 2012). FLS help to define the articular cartilage niche, contributing molecules important for lubrication, ECM turnover, and inflammation (Kiener et al., 2010). They secrete lubricin, a key component of joint lubrication that also has chondroprotective (Jay, 1992; Jay et al., 2000; Jay et al., 2007) and cell anti-adhesive properties (Rhee et al., 2005). FLS also synthesize HA (Jay et al., 2007) which has been suggested to interact with synovial fluid lipids in hydration lubrication (Lin et al., 2020). Additionally, FLS both respond to and contribute to the secretion of inflammatory cytokines (Kiener et al., 2010) and respond to shear loading (Sun et al., 2003).

The synovium is recognized as a source of cells capable of chondrogenesis *in vivo* (Kurth et al., 2011), and recent lineage tracing studies in mice have reported that GDF5-lineage cells – which include synoviocytes and other cells derived from the joint interzone during development – and in particular cells likely derived from the synovium, can migrate to articular cartilage defects as part of a large-scale injury response where they produce repair tissue of variable quality (Decker et al., 2017; Roelofs et al., 2017). We contend that the migration of synoviocytes is not in question at this juncture, though the healing capacity of migrating synovial cells in response to full-thickness cartilage defects is currently unknown (Chagin and Medvedeva, 2017). This study focuses on the capacity of these synovial cells to perform normal 'wear and tear' maintenance. Here, we undertake a series of *in vitro* studies to establish the feasibility of this paradigm. Critical underlying experiments confirm a) chondrocytes die in response to physiologic loading, b) FLS become dislodged from synovium by physiologic joint loading and attach to abraded cartilage, and c) FLS modulate their behavior upon direct interaction with chondrocytes and when attached to cartilage.

2. Methods

2.1. Cell and tissue isolation and culture

Human FLS were isolated from the synovium of three male cadavers (age 28.3 ± 8.3 years; MTF Biologics, Edison, NJ) and four males undergoing total knee arthroplasty (age 69.5 ± 6.0 years) via digestion with collagenase type II (Worthington). Unless otherwise noted, FLS were cultured as previously described (Stefani et al., 2019). Single-donor cultures were grown for at least two passages to remove non-FLS subpopulations (Sampat et al., 2011; Silverstein et al., 2017). Cells were then pooled and grown for at least one additional passage before testing.

Human articular chondrocytes (AC) were isolated from articular cartilage shavings of one cadaver (MTF Biologics, Edison, NJ) via digestion with collagenase type II. Unless otherwise noted, AC were cultured as previously described (Lee et al., 2021). AC were assayed at passages 3–4.

Bovine synovium and cartilage explants were harvested from the tibiofemoral joints of calves (2–4 weeks old) acquired from a local abattoir (Institutional Animal Care and Use Committee-exempt) and were maintained in a chemically-defined medium consisting of DMEM supplemented with 50 μg/mL L-proline, 100 μg/mL sodium pyruvate, 1 % ITS Premix (Corning), and 1 % antibiotic–antimycotic until assayed. Bovine FLS (jbFLS) were isolated using the same method as human FLS.

2.2. Contact shear and cell transfer assays

2.2.1. Cartilage-on-cartilage friction

Bovine femoral condylar cartilage biopsy punches and tibial cartilage strips were harvested and loaded onto a custom-built friction tester (Krishnan et al., 2004) where they were loaded for 2 h (1 mm/s, 907 g load corresponding to an average stress of 409 kPa, 5 mm total path length) in a bath of 50 % synovial fluid (Animal Technologies) in DMEM at 37 °C (Fig. 1A). Punches were then used for viability staining and imaging; mapping of local elastic moduli and topography via atomic force microscopy (AFM); or histological staining. The applied load was determined by targeting the low end of loading experienced by knee joint articular cartilage during normal activity (Ahmed and Burke, 1983; Ahmed et al., 1983), using the Fuji Film method to determine contact area (Ateshian et al., 1994).

Viability staining was performed using calcein-AM (green, live cells, Invitrogen) and ethidium homodimer-1 (red, dead cells) (Invitrogen). Images were acquired on a Zeiss LSM 700 inverted confocal microscope. Fluorescence intensities were quantified in a line through the depth of the tissue using ImageJ (Chahine et al., 2007).

For mapping of elastic moduli and topography, tissues were frozen, 300 μm sections were taken from the SZ using a sledge cryotome, and sections were mounted to glass slides. Tissue sections were tested (n = 3 slides per group) using an Asylum MFP-3D AFM with a spherical polystyrene probe tip (1.8 μm radius, sQube CP-FM-PS-B). Fast force mapping mode sampling at 100 Hz with a 1 μN trigger force across a 120 μm by 120 μm region was used to acquire maps of local elastic moduli and topography. Single force-indentation curves were obtained and fitted to a Hertz model of elasticity to determine the elastic modulus (Radmacher et al., 1996).

For histological analyses, tissues were fixed in 4 % paraformaldehyde, embedded in paraffin, sectioned (6 μm thickness), and stained. General tissue staining was performed using hematoxylin and eosin. Lubricin (PRG4) was probed with a primary mouse anti-lubricin antibody (1:500 dilution; Millipore Sigma, MABT400) for 1 h at room temperature. Slides were developed using a mouse-specific HRP/DAB staining kit (Abcam ab64259), with hematoxylin used as a counterstain.

2.2.2. Synovium-on-glass cell detachment

Bovine synovial explants were mounted onto 8-mm platens with rubber backing and loaded with friction against glass for five hours with a compressive stress of 100 kPa (1 mm/s, 5 mm path length) in a bath containing 50 % synovial fluid in media (Estell et al., 2021). Baths were removed after every hour and centrifuged to retrieve cells. Cell pellets were resuspended and stained with the vital stain trypan blue. Live and dead cells were counted to determine cell release and viability over time.

2.2.3. FLS attachment to cartilage

Cells were isolated via collagenase digestion of bovine synovium and immediately loaded with the lipid-membrane dye DiO, while tibial cartilage strips were loaded with Hoescht 33342. 500 k jbFLS were then parachuted onto the tibial strips in serum-free, chemically-defined medium. Cultures were incubated for 24 h. 2 mm punches were taken from the friction-abraded region or matched control locations and imaged on a confocal microscope.

2.3. Intracellular calcium signaling assay

Human FLS were loaded in suspension with the intracellular Ca^{2+} dye Fura Red-AM (ThermoFisher Scientific) at 5 μM for 40 min before being parachuted onto collagen-coated glass slides with or without a confluent monolayer of human AC (n = 5 slides per group) (Fig. 3**A**). Cultures were incubated for 4 h at 37 °C to allow for cell attachment before testing.

Calcium signaling assays were performed as previously described (Estell et al., 2017). Briefly, slides were loaded into a parallel plate flow chamber and left to equilibrate on the microscope stage for 10 min. A 6-minute time-lapse consisting of 2 min each of pre-flow baseline, flow, and post-flow observation was then acquired. Experiments were performed in Hank's balanced salt solution supplemented with 0.5 % FBS, and flow was applied at 0.05 Pa to induce calcium signaling without

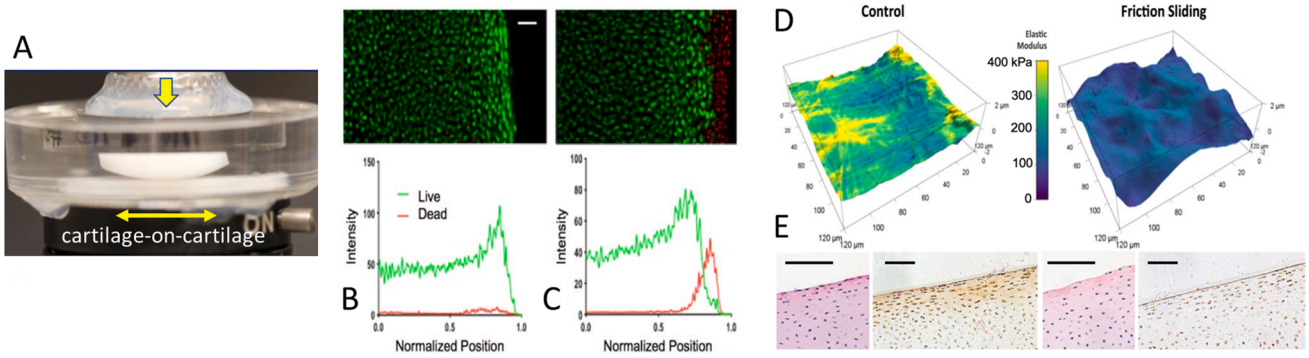

Fig. 1. A) Reciprocal friction shear loading of articular cartilage. B) Representative viability staining of B) unloaded and C) loaded cartilage with corresponding red and green fluorescence channel intensity, SZ on right. Bar: 50 μm. D) AFM Imaging of Cartilage Surface. Topography, Roughness (RQ, scale ± 2 μm), and Hertz elastic modulus plot of cartilage surface (scale: 0–400 kPa) of control and after 2 h of physiologic friction loading. E) H&E and PRG4 staining (brown) of juvenile bovine cartilage, control (2 images at left) and after friction loading (2 images at right) at 409 kPa for 2 h, showing decreased superficial lubricin after shear and possible loss of surface lining chondrocytes. Scale bar: 100 μm. (For interpretation of the references to colour in this figure legend, the reader is referred to the web version of this article.)

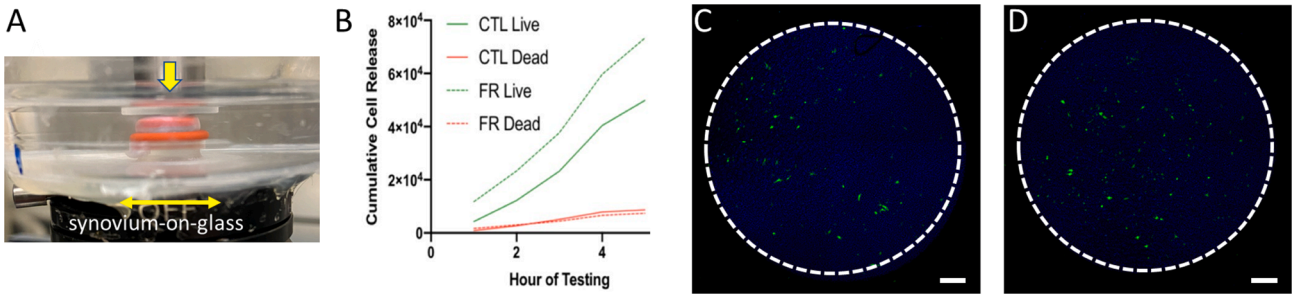

Fig. 2. A) Reciprocal shear loading of synovium on glass. B) Quantification of release of synovial cells, living (calcein) and dead (ethidium homodimer), into a bath of media:synovial fluid (1:1). FLS (green) attachment to C) control and D) friction shear-loaded articular cartilage plugs (chondrocyte nuclei labeled blue). N = 4 cartilage plugs for each condition. Scale bar: 200 μm. (For interpretation of the references to colour in this figure legend, the reader is referred to the web version of this article.)

causing cell detachment.

Fluorescence tracings were acquired for 100 cells per slide and were processed using a custom MATLAB script. Responders were defined as cells for which calcium transients increased by at least 30 % over baseline. Peak latency was defined as the time delay between onset of flow and the calcium transient peak. The fraction of responding cells per slide and peak latencies were analyzed using two-way analysis of variance with Tukey's HSD post-hoc test ($\alpha = 0.05$).

2.4. Dye-transfer assay, flow cytometry, and AFM

Human AC were plated in a 12-well plate and grown until highly confluent. On the day of the assay, FLS were loaded with 2 mM calcein-AM, and the AC monolayer was stained with the lipid-membrane stain DiI (Invitrogen). 50 k FLS were parachuted onto the AC monolayer, and co-cultures were incubated for 4 h. Cells were then harvested and kept on ice until analyzed by flow cytometry.

Cells were passed through a 70 μm strainer and loaded into a flow cytometer (FACScalibur, BD Biosciences), where they were excited by a 488 nm laser and read on the forward scatter, side scatter, FL1 (calcein, 530/30), and FL2 (DiI, 585/42) channels.

For AFM measurements, FLS were grown to confluence in a collagen-coated 60 mm dish prior to analysis. Fast force mapping was performed as for cartilage sections but using a colloidal probe tip (6.1 μm diameter, NanoAndMore) and sampling at 50 Hz.

2.5. COL2A1 reporter cell line

Pooled human FLS and jbFLS were transduced with a lentiviral expression vector encoding tdTomato (red) driven by the *COL2A1* promoter and GFP (green) driven by the constitutive EF-1α promoter (kindly provided by Dr. Glyn D. Palmer, University of Florida). Transduced human FLS were parachuted onto mature tissue-engineered cartilage constructs (Lima et al., 2007) and were cultured in chondrogenic media consisting of DMEM supplemented with 50 μg/mL L-proline, 100 μg/mL sodium pyruvate, 1 % ITS Premix (Corning), and 1 % antibiotic–antimycotic for 10 days before imaging on a confocal microscope. Image processing and quantification was performed in MATLAB. Bovine cells were treated similarly but were parachuted on bovine tibial explant cartilage and cultured for 3 days.

3. Results

3.1. Cartilage-on-cartilage friction loading caused SZ damage

The effects of cartilage-on-cartilage friction loading (Fig. 1**A**) were evaluated by imaging to assess cell viability and ECM loss and by AFM to assess changes in mechanical properties and topography of the SZ. Relative to control, friction loading caused an increase in cell death in the SZ (Fig. 1**B-C**). Notably, cell death was confined to the SZ, with no loss of viability in deeper zones. Loading also caused a loss of PRG4 and ECM at the SZ as evidenced by a decrease in staining intensity (Fig. 1**E**). Friction led to a decrease in elastic modulus (control: 272 ± 14 kPa vs friction: 95 ± 16 kPa, $p = 0.0002$, $n = 3$) at the tissue surface and increased roughness (control: 217 ± 82 nm vs friction: 667 ± 476 nm, $p = 0.18$, $n = 3$) as compared to unloaded controls (Fig. 1**D**).

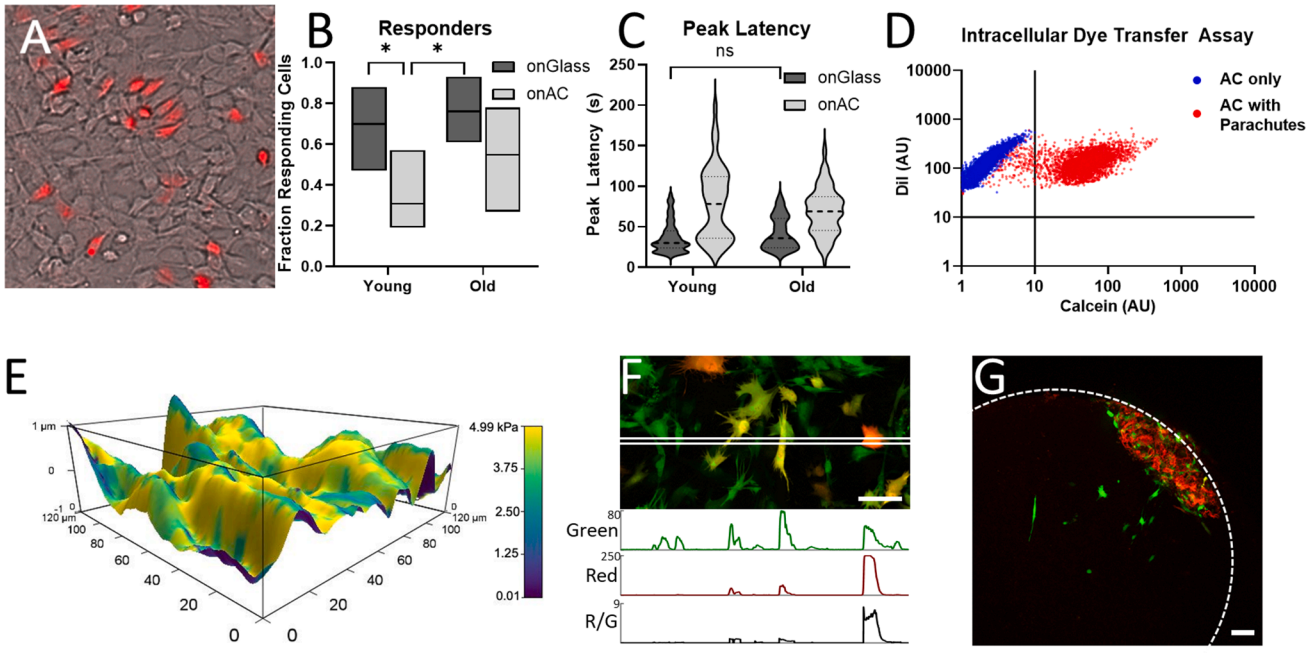

Fig. 3. A) FLS parachuted (Fura-red dye- red) on articular chondrocyte (AC) monolayer. B) Fraction of responding cells. FLS parachuted on an AC monolayer showed a significant decrease in response rate for young pool cells (n = 5 slides each, p = 0.026). C) Peak latencies of responding cells. All comparisons not marked "ns" are significant, with p < 0.001. D) Dye transfer from FLS to articular chondrocyte monolayer quantified with flow cytometry. Cells in the upper-left quadrant were DiI+/Calcein-, indicating no dye transfer has occurred, and cells in the upper-right quadrant were DiI+/Calcein+, indicating that dye transfer has occurred. E) AFM imaging of articular cartilage monolayer revealed a non-uniform substrate both in terms of topography and elastic modulus F) *COL2A1* reporter human cells parachuted on engineered cartilage. Cellular morphology was non-uniform, and *COL2A1* expression levels (red fluorescence) varied. Below image, pixel intensity for GFP (green, successfully transduced cells), tdTomato (red, cells expressing *COL2A1*), and the red:green ratio. Scale bar: 100 μm. G) *COL2A1* reporter bovine cells on cartilage explant. Cells localized to a suspected defect site where they expressed *COL2A1*. Scale bar: 100 μm. (For interpretation of the references to colour in this figure legend, the reader is referred to the web version of this article.)

3.2. Synovial cells detached from the synovium under friction loading and attached to cartilage

The release of synovial cells from explant tissue under shear stress was evaluated using a custom friction bioreactor under physiologic loading conditions (Fig. 2**A**). Cell release into the media was elevated under friction when compared to static controls (Fig. 2**B**). While cells released from synovium by friction were capable of attachment to cartilage (data not shown), the quantity of cells retrieved was suboptimal to perform quantitative parachute studies. As such, fluorescently-labeled cells freshly digested from tissue were parachuted onto intact and friction shear-loaded cartilage. FLS could attach under both conditions, but attachment increased slightly for loaded cartilage (per 2 mm punch, control: 72 ± 16 cells vs friction: 99 ± 22 cells, p = 0.099, n = 4; Fig. 2**C-D**).

3.3. Direct interaction with an AC monolayer modulated FLS mechanosensitivity to fluid shear

The effects of parachute co-culture and age on FLS mechanosensitivity in response to fluid shear were assessed by measurement of intracellular calcium signaling (Fig. 3**A**). The parachute substrate (glass vs AC) was a significant factor (p = 0.0032) while cell age (p = 0.10) and the interaction (p = 0.32) were not significant. FLS parachuted onto chondrocyte monolayers responded to fluid shear at a decreased rate, significantly so for young cells (30.8 ± 15.4 % vs 69.8 ± 20.5 %, p = 0.026) (Fig. 3**B**). For peak latency – the time between flow onset and calcium peak – substrate (p < 0.0001) and the interaction (p < 0.0001) were significant, while age was not (p = 0.12) (Fig. 3**C**). For cells plated on glass, response times were largely unimodal, with 90 % of young cells responding within 69 s of flow onset. Cells plated on the AC monolayer responded bimodally, with approximately half of responders reaching peak signal with latency similar to those plated on glass, while the other half reached peak much later.

To better understand the mechanical microenvironment the parachuted FLS experience, AFM was used to map AC monolayer topography and elastic modulus (Fig. 3**E**). Relative to glass – which is smooth and stiff, with a Young's modulus of 70 GPa – AC monolayers were uneven and had elastic moduli of < 5 kPa.

3.4. Parachute FLS participated in direct cell-cell communication with AC monolayer

The potential for direct intercellular communication between parachuted FLS and ACs in monolayer culture was assessed via a dye transfer assay (Fig. 3**D**). Dye-loaded FLS were able to transfer dye to 90.7 ± 0.3 % of ACs.

3.5. Expression of COL2A1 in cartilage-attached FLS was variable

In order to assess chondrogenic differentiation in cartilage-attached FLS, *COL2A1* reporter-labeled cells were parachuted onto engineered or explant cartilage and allowed to differentiate in culture before assessment. *COL2A1* expression, as measured by tdTomato signal relative to GFP signal, was variable in human cells (Fig. 3**F**). Interestingly, on one explant, jbFLS were observed to concentrate at a location on the edge of the tissue where they exhibited high expression of *COL2A1* (Fig. 3**G**). We suspect the cells migrated to a site of tissue damage caused by punching, but further study is needed to assess the implications of such activity.

4. Discussion

In the studies presented, we provide support for our 'wear and tear' paradigm, which shifts the focus from cartilage's poor healing capacity in response to significant injury to the joint's response to regular sub-injurious cartilage damage. This shift is motivated by the tissue's ability to bear load for the majority of an individual's life despite consistent mechanical wear. A prevailing school of thought is that this 'wear and tear' in normal adult cartilage is compensated by the turnover of the matrix components synthesized by chondrocytes (Goldring and Marcu, 2009). In cartilage degeneration or OA, catabolism exceeds the anabolic capacities of chondrocytes, the cartilage matrix degenerates, and the joint cartilage gets damaged (Aigner et al., 2006). We contend that chondrocytes are lost in the process of 'wear and tear', as suggested by Clements et al. (2001), and are therefore unable to maintain tissue homeostasis in the vicinity of SZ microdamage (Bonnevie et al., 2018; Horisberger et al., 2013; Waller et al., 2012).

Normal situations of excessive loading may lead to elevated cell death, while activities of daily living produce much less cell death. The repair mechanism we propose could replace dead cells when loading is excessive (but non-injurious), but it would not be immediate. While this repair takes place and dead SZ cells are replaced by cells of synovial origin, we argue that the tissue can fulfill its main load-bearing and lubrication functions.

Tissue explant and cell culture studies provide invaluable tools for musculoskeletal research that are complementary to *in vivo* animal models. Various loading configurations have been used to study friction shear loading of cartilage (Waller et al., 2012). Sliding of glass-on-cartilage has yielded elegant studies of depth-dependent shear properties of cartilage which have shown preferential cell necrosis at the top surface of the SZ and apoptosis in lower regions of the SZ (Bonnevie et al., 2011; Bonnevie et al., 2018), (Fig. 1**B-C).** The current studies were undertaken as no groups have rigorously investigated the mechanism(s) by which cartilage can maintain its function before degenerating despite this cell loss.

The *in vitro* studies performed herein suggest that cartilage subjected to physiologic loading sustains local SZ chondrocyte death (Fig. 1**B-C)** and tissue microdamage (Fig. 1**D-E**), similar to results reported *in vivo* in rabbits (Horisberger et al., 2013). Though cell death is more pronounced in our *in vitro* studies, this is unlikely due to changes in friction properties, as the study was performed under migrating contact conditions which maintain a very low friction coefficient for the duration of the test (Caligaris and Ateshian, 2008).

The synovium is a reservoir of FLS and is an attractive candidate cell source for cartilage repair due to its location near to and physical overlap with cartilage (Hunziker and Rosenberg, 1996; Kurth et al., 2011; Roelofs et al., 2017). This physical contact may provide a means for transfer of FLS to the cartilage surface by providing friction forces which lead to detachment of cells (Fig. 2**B)** that adhere readily to the cartilage surface (Fig. 2**C-D**). Fragments of synovium and synovial cells are found in the synovial fluid of both healthy and diseased joints (Jones et al., 2008), providing a route to the cartilage surface. These conditions make the synovium an appealing candidate for maintaining homeostasis of articular cartilage under normal conditions.

FLS are sensitive to mechanical loading (Estell et al., 2017; Ingram et al., 2008; Sun et al., 2003) and can communicate with each other (Estell et al., 2017; Gupta et al., 2014) and chondrocytes (Fig. 3**D**) via gap junctions (D'Andrea et al., 1998). Chondrocytes may play a role in the behavior of hFLS, which otherwise behave similarly to other types of MSCs (Sampat et al., 2011). The dye transfer assay reflects a combination of direct FLS-AC transfer and subsequent transfer among ACs within the monolayer. Dye transfer at this scale implies robust formation of intercellular junctions, which mediate communication via the transfer of proteins, peptides, and small molecules between these cell types (Carpintero-Fernandez et al., 2018; Mayan et al., 2015). Additional modulation of cell behavior could be caused by signaling pathways that require cell–cell contact, such as Notch, which has been shown to play an important role in determining FLS identity (Wei et al., 2020). The bimodal calcium response of FLS on the AC monolayer (Fig. 3**C**) suggests either a mixed population of cells or multiple response modes to the same stimulus; this behavior is not observed in FLS directly attached to glass slides. Differences in glass and AC substrate mechanical properties may also contribute to the disparate calcium response, as substrate stiffness has been shown to influence cell behavior and differentiation in MSCs (Engler et al., 2006). Hinting at intrinsic age-related changes of FLS, under the conditions of the current study, FLS age appears to modulate substrate-dependent calcium signaling on glass and AC monolayers, as the changes in calcium response caused by changes in substrate were diminished for older FLS.

In these studies, we have established the feasibility of early events that would precede subsequent maintenance/repair of cartilage by FLS, which remains to be demonstrated. In this context, FLS-derived ECM has been reported to create a microenvironment that supports FLS expansion with enhanced chondrogenic potential (He et al., 2009; Li and Pei, 2018) which may provide positive feedback during repair. Our reporter studies of FLS indicate that while the chondrogenic phenotype is generally associated with a rounded morphology without attachment (Benya and Shaffer, 1982), FLS here show elevated *COL2A1* expression – a hallmark of chondrogenesis – despite attachment and flattened/spread morphology. Moreover, studies have suggested that FLS represent the best MSC candidate for cartilage regeneration as they exhibit the greatest chondrogenic potential and the least hypertrophic differentiation (Jones and Pei, 2012; Sakaguchi et al., 2005). Intra-articular FLS injections can enhance repair of partial thickness cartilage defects in the pig, (Pei et al., 2013) and tissue-engineered cartilage made with FLS achieved native mechanical properties and GAG composition (Alegre-Aguaron et al., 2014; Sampat et al., 2013; Sampat et al., 2011).

The joint environment is biochemically and mechanically complex, and the work presented here is limited in that it captures only a fraction of the cues cells encounter *in vivo*. Moreover, while these studies demonstrate the feasibility of FLS-mediated repair of 'wear and tear', we cannot conclude that it occurs *in vivo* or the importance of such a response, should it exist. To address these limitations, biofidelic *in vitro* systems permitting long-term monitoring of cartilage-synovium co-culture with physiologic loading can be employed (Gangi et al., 2022). In addition, future experiments assessing interactions of cartilage and synovium from young and adult donors can elucidate if cartilage erosion from 'wear and tear' is more a consequence of the synovium's diminished capacity to maintain homeostasis of the cartilage surface rather than exclusively intrinsic changes to cartilage and chondrocytes.

5. Funding

This work was supported in part by NIH grants 1R01AR68133, R21AR075245, 5P41EB027062, R01AR077760, R21AR080516 and the Orthopedic Scientific Research Foundation.

6. Conflict of interest statement

Clark T. Hung discloses the following: Royalties from the Musculoskeletal Transplant Foundation, Honorarium for Associate Editor of the Journal of Orthopedic Research, and Editor of Orthopedic Research and Reviews.

CRediT authorship contribution statement

Matthew J. Pellicore: . **Lianna R. Gangi:** Writing – review & editing, Visualization, Methodology, Investigation, Formal analysis. **Lance A. Murphy:** Writing – review & editing, Visualization, Investigation. **Andy J. Lee:** Writing – review & editing, Visualization, Investigation. **Timothy Jacobsen:** Writing – review & editing, Visualization, Methodology, Investigation. **Hagar M. Kenawy:** Writing – review &

editing, Visualization, Investigation. **Roshan P. Shah:** Writing – review & editing, Resources. **Nadeen O. Chahine:** Writing – review & editing, Supervision, Conceptualization. **Gerard A. Ateshian:** Writing – review & editing, Supervision, Conceptualization. **Clark T. Hung:** Writing – review & editing, Writing – original draft, Supervision, Project administration, Funding acquisition, Conceptualization.

Declaration of Competing Interest

The authors declare that they have no known competing financial interests or personal relationships that could have appeared to influence the work reported in this paper.

References

Ahmed, A.M., Burke, D.L., 1983. In-vitro measurement of static pressure distribution in synovial joints - part I: tibial surface of the knee. J. Biomech. Eng. 105, 216–225.

Ahmed, A.M., Burke, D.L., Yu, A., 1983. In-vitro measurement of static pressure distribution in synovial joints - part II: retropatellar surface. J. Biomech. Eng. 105, 226–236.

Aigner, T., Soeder, S., Haag, J., 2006. IL-1beta and BMPs–interactive players of cartilage matrix degradation and regeneration. Eur. Cell Mater. 12, 49–56 discussion 56.

Alegre-Aguaron, E., Sampat, S.R., Xiong, J.C., Colligan, R.M., Bulinski, J.C., Cook, J.L., Ateshian, G.A., Brown, L.M., Hung, C.T., 2014. Growth factor priming differentially modulates components of the extracellular matrix proteome in chondrocytes and synovium-derived stem cells. Plos One 9, e88053.

Ateshian, G.A., Kwak, S.D., Soslowsky, L.J., Mow, V.C., 1994. A stereophotogrammetric method for determining in situ contact areas in diarthrodial joints, and a comparison with other methods. J. Biomech. 27, 111–124.

Benya, P.D., Shaffer, J.D., 1982. Dedifferentiated chondrocytes reexpress the differentiated collagen phenotype when cultured in agarose gels. Cell 30, 215–224.

Bonnevie, E.D., Baro, V., Wang, L., Burris, D.L., 2011. In-situ studies of cartilage microtribology: roles of speed and contact area. Tribol. Lett. 41, 83–95.

Bonnevie, E.D., Delco, M.L., Bartell, L.R., Jasty, N., Cohen, I., Fortier, L.A., Bonassar, L.J., 2018. Microscale frictional strains determine chondrocyte fate in loaded cartilage. J. Biomech. 74, 72–78.

Buckley, M.R., Gleghorn, J.P., Bonassar, L.J., Cohen, I., 2008. Mapping the depth dependence of shear properties in articular cartilage. J. Biomech. 41, 2430–2437.

Caligaris, M., Ateshian, G.A., 2008. Effects of sustained interstitial fluid pressurization under migrating contact area, and boundary lubrication by synovial fluid, on cartilage friction. Osteoarthrit. Cartil. / OARS, Osteoarthrit. Res. Soc. 16, 1220–1227.

Carpintero-Fernandez, P., Gago-Fuentes, R., Wang, H.Z., Fonseca, E., Caeiro, J.R., Valiunas, V., Brink, P.R., Mayan, M.D., 2018. Intercellular communication via gap junction channels between chondrocytes and bone cells. Biochim. Biophys. Acta Biomembr. 1860, 2499–2505.

Chagin, A.S., Medvedeva, E.V., 2017. Cartilage stem cells identified, but can they heal? Nat. Rev. Rheumatol. 13, 522–524.

Chahine, N.O., Ateshian, G.A., Hung, C.T., 2007. The effect of finite compressive strain on chondrocyte viability in statically loaded bovine articular cartilage. Biomech. Model. Mechanobiol. 6, 103–111.

Clements, K.M., Bee, Z.C., Crossingham, G.V., Adams, M.A., Sharif, M., 2001. How severe must repetitive loading be to kill chondrocytes in articular cartilage? Osteoarthrit. Cartil. / OARS, Osteoarthrit. Res. Soc. 9, 499–507.

D'Andrea, P., Calabrese, A., Grandolfo, M., 1998. Intercellular calcium signalling between chondrocytes and synovial cells in co-culture. Biochem. J. 329 (Pt 3), 681–687.

Decker, R.S., Um, H.B., Dyment, N.A., Cottingham, N., Usami, Y., Enomoto-Iwamoto, M., Kronenberg, M.S., Maye, P., Rowe, D.W., Koyama, E., Pacifici, M., 2017. Cell origin, volume and arrangement are drivers of articular cartilage formation, morphogenesis and response to injury in mouse limbs. Dev. Biol. 426, 56–68.

Engler, A.J., Sen, S., Sweeney, H.L., Discher, D.E., 2006. Matrix elasticity directs stem cell lineage specification. Cell 126, 677–689.

Estell, E.G., Murphy, L.A., Silverstein, A.M., Tan, A.R., Shah, R.P., Ateshian, G.A., Hung, C.T., 2017. Fibroblast-like synoviocyte mechanosensitivity to fluid shear is modulated by interleukin-1alpha. J. Biomech. 60, 91–99.

Estell, E.G., Murphy, L.A., Gangi, L.R., Shah, R.P., Ateshian, G.A., Hung, C.T., 2021. Attachment of cartilage wear particles to the synovium negatively impacts friction properties. J. Biomech. 127, 110668.

Gangi, L.R., Petersen, C.A., Oungoulian, S.R., Estell, E.G., Durney, K.M., Suh, J.T., Ateshian, G.A., Hung, C.T., 2022. A Friction Testing-Bioreactor Device for Study of Synovial Joint Biomechanics. Mechanobiology, and Physical Regulation. J Vis Exp.

Goldring, M.B., Marcu, K.B., 2009. Cartilage homeostasis in health and rheumatic diseases. Arthritis Res. Ther. 11, 224.

Gupta, A., Niger, C., Buo, A.M., Eidelman, E.R., Chen, R.J., Stains, J.P., 2014. Connexin43 enhances the expression of osteoarthritis-associated genes in synovial fibroblasts in culture. BMC Musculoskelet. Disord. 15, 425.

He, F., Chen, X., Pei, M., 2009. Reconstruction of an in vitro tissue-specific microenvironment to rejuvenate synovium-derived stem cells for cartilage tissue engineering. Tissue Eng. Part A 15, 3809–3821.

Horisberger, M., Fortuna, R., Leonard, T.R., Valderrabano, V., Herzog, W., 2012. The influence of cyclic concentric and eccentric submaximal muscle loading on cell viability in the rabbit knee joint. Clin. Biomech. (Bristol, Avon) 27, 292–298.

Horisberger, M., Fortuna, R., Valderrabano, V., Herzog, W., 2013. Long-term repetitive mechanical loading of the knee joint by in vivo muscle stimulation accelerates cartilage degeneration and increases chondrocyte death in a rabbit model. Clin. Biomech. (Bristol, Avon) 28, 536–543.

Hui, A.Y., McCarty, W.J., Masuda, K., Firestein, G.S., Sah, R.L., 2012. A systems biology approach to synovial joint lubrication in health, injury, and disease. Wiley interdisciplinary reviews. Syst. Biol. Med. 4, 15–37.

Hunziker, E.B., Rosenberg, L.C., 1996. Repair of partial-thickness defects in articular cartilage: cell recruitment from the synovium. J. Bone Jt. Surg. Am. 78-A, 721–733.

Ingram, K.R., Wann, A.K., Angel, C.K., Coleman, P.J., Levick, J.R., 2008. Cyclic movement stimulates hyaluronan secretion into the synovial cavity of rabbit joints. J. Physiol. 586, 1715–1729.

Jay, G.D., 1992. Characterization of a bovine synovial fluid lubricating factor. I. chemical, surface activity and lubricating properties. Connect Tissue Res. 28, 71–88.

Jay, G.D., Britt, D.E., Cha, C.J., 2000. Lubricin is a product of megakaryocyte stimulating factor gene expression by human synovial fibroblasts. J. Rheumatol. 27, 594–600.

Jay, G.D., Torres, J.R., Rhee, D.K., Helminen, H.J., Hytinnen, M.M., Cha, C.J., Elsaid, K., Kim, K.S., Cui, Y., Warman, M.L., 2007. Association between friction and wear in diarthrodial joints lacking lubricin. Arthritis Rheum. 56, 3662–3669.

Jones, E.A., Crawford, A., English, A., Henshaw, K., Mundy, J., Corscadden, D., Chapman, T., Emery, P., Hatton, P., McGonagle, D., 2008. Synovial fluid mesenchymal stem cells in health and early osteoarthritis: detection and functional evaluation at the single-cell level. Arthritis Rheum. 58, 1731–1740.

Jones, B.A., Pei, M., 2012. Synovium-derived stem cells: a tissue-specific stem cell for cartilage engineering and regeneration. Tissue Eng. Part B Rev. 18, 301–311.

Kiener, H.P., Watts, G.F., Cui, Y., Wright, J., Thornhill, T.S., Skold, M., Behar, S.M., Niederreiter, B., Lu, J., Cernadas, M., Coyle, A.J., Sims, G.P., Smolen, J., Warman, M. L., Brenner, M.B., Lee, D.M., 2010. Synovial fibroblasts self-direct multicellular lining architecture and synthetic function in three-dimensional organ culture. Arthritis Rheum. 62, 742–752.

Krishnan, R., Caligaris, M., Mauck, R.L., Hung, C.T., Costa, K.D., Ateshian, G.A., 2004. Removal of the superficial zone of bovine articular cartilage does not increase its frictional coefficient. Osteoarthrit. Cartil. / OARS, Osteoarthrit. Res. Soc. 12, 947–955.

Kurth, T.B., Dell'accio, F., Crouch, V., Augello, A., Sharpe, P.T., De Bari, C., 2011. Functional mesenchymal stem cell niches in adult mouse knee joint synovium in vivo. Arthritis Rheum. 63, 1289–1300.

Lee, A.J., Mahoney, C.M., Cai, C.C., Ichinose, R., Stefani, R.M., Marra, K.G., Ateshian, G. A., Shah, R.P., Vunjak-Novakovic, G., Hung, C.T., 2021. Sustained delivery of SB-431542, a Type I TGF-β1 receptor inhibitor, to prevent arthrofibrosis. Tissue Eng. A 27, 1411–1421.

Li, J., Pei, M., 2018. A protocol to prepare decellularized stem cell matrix for rejuvenation of cell expansion and cartilage regeneration. Methods Mol. Biol. 1577, 147–154.

Lima, E.G., Bian, L., Ng, K.W., Mauck, R.L., Byers, B.A., Tuan, R.S., Ateshian, G.A., Hung, C.T., 2007. The Beneficial Effect of Delayed Compressive Loading on Tissue-Engineered Cartilage Constructs Cultured with TGF-β3. Osteoarthritis Cartilage 15, 1025–1033.

Lin, W., Liu, Z., Kampf, N., Klein, J., 2020. The role of hyaluronic acid in cartilage boundary lubrication. Cells 9.

Mayan, M.D., Gago-Fuentes, R., Carpintero-Fernandez, P., Fernandez-Puente, P., Filgueira-Fernandez, P., Goyanes, N., Valiunas, V., Brink, P.R., Goldberg, G.S., Blanco, F.J., 2015. Articular chondrocyte network mediated by gap junctions: role in metabolic cartilage homeostasis. Ann. Rheum. Dis. 74, 275–284.

Neu, C.P., Reddi, A.H., Komvopoulos, K., Schmid, T.M., Di Cesare, P.E., 2010. Increased friction coefficient and superficial zone protein expression in patients with advanced osteoarthritis. Arthritis Rheum. 62, 2680–2687.

Oungoulian, S.R., Durney, K.M., Jones, B.K., Ahmad, C.S., Hung, C.T., Ateshian, G.A., 2015. Wear and damage of articular cartilage with friction against orthopedic implant materials. J. Biomech. 48, 1957–1964.

Pei, M., He, F., Li, J., Tidwell, J.E., Jones, A.C., McDonough, E.B., 2013. Repair of large animal partial-thickness cartilage defects through intraarticular injection of matrix-rejuvenated synovium-derived stem cells. Tissue Eng. Part A 19, 1144–1154.

Radmacher, M., Fritz, M., Kacher, C.M., Cleveland, J.P., Hansma, P.K., 1996. Measuring the viscoelastic properties of human platelets with the atomic force microscope. Biophys. J. 70, 556–567.

Rhee, D.K., Marcelino, J., Baker, M., Gong, Y., Smits, P., Lefebvre, V., Jay, G.D., Stewart, M., Wang, H., Warman, M.L., Carpten, J.D., 2005. The secreted glycoprotein lubricin protects cartilage surfaces and inhibits synovial cell overgrowth. J. Clin. Invest. 115, 622–631.

Roelofs, A.J., Zupan, J., Riemen, A.H.K., Kania, K., Ansboro, S., White, N., Clark, S.M., De Bari, C., 2017. Joint morphogenetic cells in the adult mammalian synovium. Nat. Commun. 8, 15040.

Roemhildt, M.L., Beynnon, B.D., Gardner-Morse, M., Badger, G., Grant, C., 2012. Changes induced by chronic in vivo load alteration in the tibiofemoral joint of mature rabbits. J. Orthop. Res. 30, 1413–1422.

Sakaguchi, Y., Sekiya, I., Yagishita, K., Muneta, T., 2005. Comparison of human stem cells derived from various mesenchymal tissues: superiority of synovium as a cell source. Arthritis Rheum. 52, 2521–2529.

Sampat, S.R., O'Connell, G., Fong, J.V., Alegre-Aguaron, E., Ateshian, G.A., Hung, C.T., 2011. Growth factor priming of synovium derived stem cells for cartilage tissue engineering. Tissue Eng. Part A 17, 2259–2265.

Sampat, S.R., Dermksian, M.V., Oungoulian, S.R., Winchester, R.J., Bulinski, J.C., Ateshian, G.A., Hung, C.T., 2013. Applied osmotic loading for promoting development of engineered cartilage. J. Biomech. 46, 2674–2681.
Schinagl, R.M., Gurkis, D., Chen, C.C., Sah, R.-L.-Y., 1997. Depth-dependent confined compression modulus of full-thickness bovine articular cartilage. J. Orthop. Res. 15, 499–506.
Silverstein, A.M., Stefani, R.M., Sobczak, E., Tong, E.L., Attur, M.G., Shah, R.P., Bulinski, J.C., Ateshian, G.A., Hung, C.T., 2017. Toward understanding the role of cartilage particulates in synovial inflammation. Osteoarthrit. Cartil. / OARS, Osteoarthrit. Res. Soc. 25, 1353–1361.
Stefani, R.M., Halder, S.S., Estell, E.G., Lee, A.J., Silverstein, A.M., Sobczak, E., Chahine, N.O., Ateshian, G.A., Shah, R.P., Hung, C.T., 2019. A functional tissue engineered synovium model to study osteoarthritis progression and treatment. Tissue Eng. Part A 25, 538–553.
Sun, H.B., Nalim, R., Yokota, H., 2003. Expression and activities of matrix metalloproteinases under oscillatory shear in IL-1 stimulated synovial cells. Connect. Tissue Res. 44, 42–49.
Waller, K.A., Zhang, L.X., Fleming, B.C., Jay, G.D., 2012. Preventing friction-induced chondrocyte apoptosis: comparison of human synovial fluid and hylan G-F 20. J. Rheumatol. 39, 1473–1480.
Wei, K., Korsunsky, I., Marshall, J.L., Gao, A., Watts, G.F.M., Major, T., Croft, A.P., Watts, J., Blazar, P.E., Lange, J.K., Thornhill, T.S., Filer, A., Raza, K., Donlin, L.T., Siebel, C.W., Buckley, C.D., Raychaudhuri, S., Brenner, M.B., 2020. Notch signalling drives synovial fibroblast identity and arthritis pathology. Nature 582, 259–264.